Supplementary Information

Giant optical activity from the radiative electromagnetic interactions in plasmonic nanoantennas

Peng Wang,[a] Li Chen,[b,e] Rongyao Wang,*[a] Yinglu Ji,[c] Dawei Zhai,[a] Xiaochun Wu,[c] Yu Liu,[a] Keqiu Chen,[e] Hongxing Xu*[b,d]

[a] School of Physics, Key Laboratory of Cluster Science of Ministry of Education, Beijing Institute of Technology, Beijing,
P R China. 100081. E-mail: wangry@bit.edu.cn
[b] Institute of Physics, Chinese Academy of Sciences, Box 603-146, Beijing,
P R China. 100190. E-mail: hongxingxu@iphy.ac.cn
[c.] CAS Key Laboratory of Standardization and Measurement for Nanotechnology, National Center for Nanoscience and Technology, Beijing,
P R China. 100190
[d.] School of Physics & Technology, Wuhan University, Wuhan,
P R China. 430072
[e.] Department of Applied Physics, Hunan University, Changsha,
P R China. 410082

Experimental Section:

1. Gold nanorods (Au NRs): preparation and surface plasmon spectroscopy.

All chemicals: sodium borohydride ($NaBH_4$), hydrogen tetrachloroaurate (III) trihydrate ($HAuCl_4 \cdot 3H_2O$), cetyltrimethylammonisum bromide (CTAB), silver nitrate ($AgNO_3$), and L-ascorbic acid (AA) were purchased from Alfa and used as received.

Firstly, CTAB-capped Au seeds were synthesized by chemical reduction of HAuCl4 with NaBH4. 100 μL of 24 mM $HAuCl_4$ and 1.8 mL water were mixed with 7.5 mL of 0.1 M CTAB aqueous solution. To the mixture 0.6 mL of 0.01 M ice-cold NaBH4 was added and followed by magnetic stirring. After 3 minutes' stirring, the seed solution was kept undisturbed at 30 ℃. Secondly, the growth solution of Au NRs which consisted of CTAB (0.1 M, 100 mL), $HAuCl_4$ (25.5 mM, 1.96 mL), $AgNO_3$ (0.01 M), H_2SO_4 (0.1 M, 2 mL), and AA (0.1 M, 0.8 mL) was prepared. The volume of AgNO3 is subject to change to tune the aspect ratio of Au NRs: 0.35, 0.45 and 0.55 mL of 0.01 M $AgNO_3$ were employed to prepare Au NRs with aspect ratio of 2.1, 2.4 and 2.7, respectively. Finally, 240 μL of seed solution was added to the growth solution. 12 h later, 0.25 mL of 0.1M AA was added into the mixture and stored at 30 ℃ for 2h to grow the Au NRs. The Au NRs solution was then centrifuged at 9000 rpm for 7 min; the precipitates were collected and redispersed in deionized water. The molar concentration of Au NRs is dependent on the volume of deionized water.

The longitudinal SPR peak position of Au NRs shows linear dependence on the aspect ratios. The following equation[1] is used to estimate the aspect ratio of Au NRs (Fig. S1b):

$$\lambda_{max} = \left(53.71 \bullet R - 42.29\right) \bullet \varepsilon_m + 495.14$$

,

Where λ_{max} is the wavelength of the longitudinal SPR peak, $\varepsilon_m = 1.77$ is the dielectric constant of the surrounding medium, and R is the aspect ratio.

Representative high-resolution TEM (HRTEM) images of Au NRs with aspect ratio of ~ 2.7 (Fig. S2) were obtained using a transmission electron microscope (JEOL, JEM-2010). The mean diameter and length were 16.0 ± 2.4 nm and 43.5 ± 7.4 nm, respectively, estimated from 100 nanorods. The aspect ratio derived from the mean diameter and length is consistent with that obtained from the above equation.
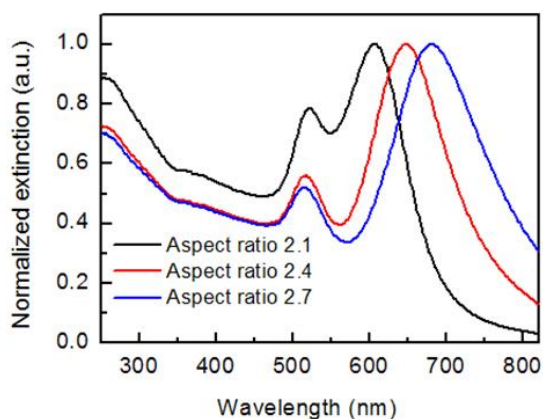
(a)
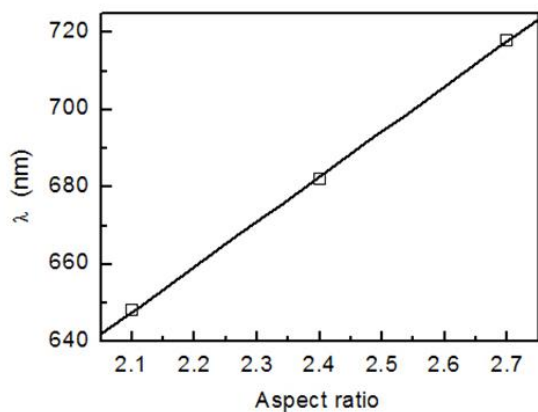
(b)

Fig. S1. (a) Normalized extinction spectra acquired from the Au NRs/CTAB colloids with different aspect ratios of ~ 2.1 (black solid line), ~ 2.4 (red solid line), and ~ 2.7 (blue solid line); (b) Correlation between longitudinal SPR peak positions (extracted from Fig. S1a) and the estimated aspect ratios.
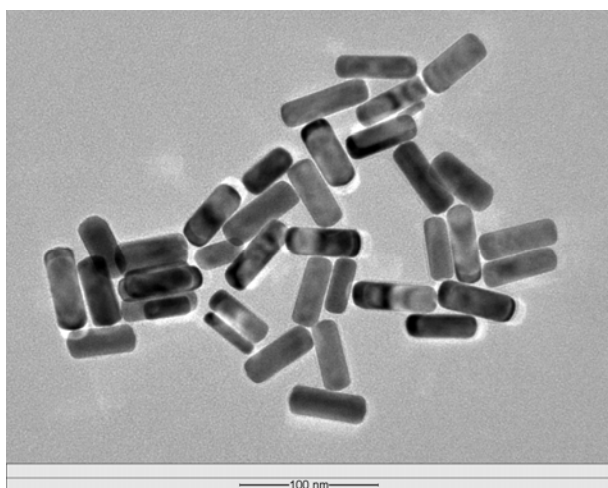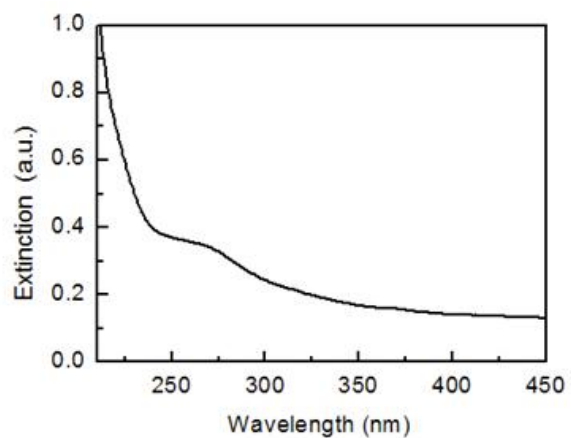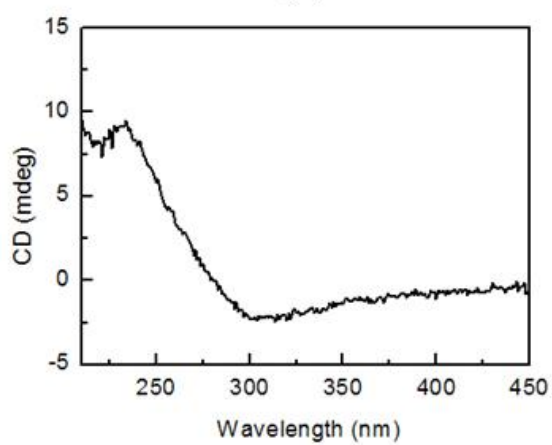

100 nm

Fig. S2. Representative TEM image of Au NRs with aspect ratio of ~ 2.7.

2. Lipid-based twisted chains of Au NRs: optical spectroscopy and structural characterization.

2.1 Lipid-based chiral template.

Fig. S3. Typical extinction (a) and CD (b) spectra of the chiral CTAB/lipid template.
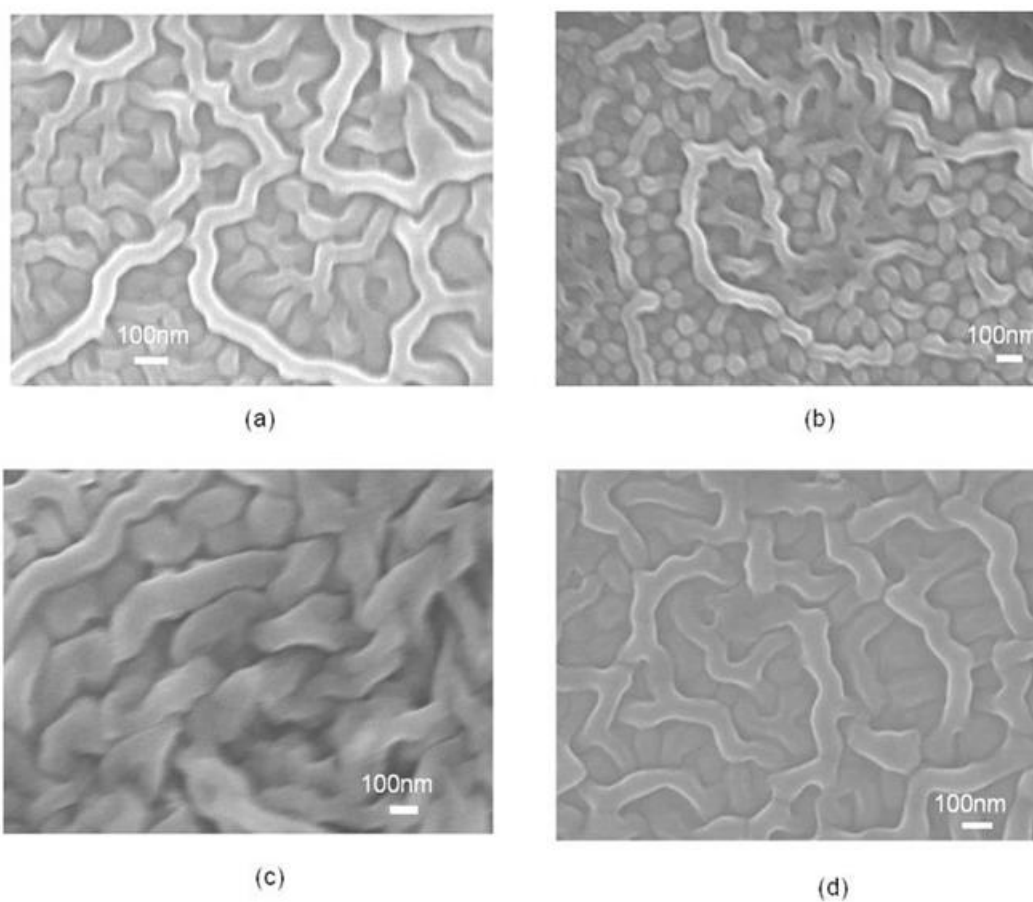
Fig. S4. SEM image obtained from the dried sample with a treatment of gold sputter-coating (30 mA, 20 s) for chiral CTAB/lipid templates (a), lipid-based linear chains of Au NRs with aspect ratio of ~2.1 (b), aspect ratio of ~2.4 (c), and aspect ratio of ~2.7 (d).

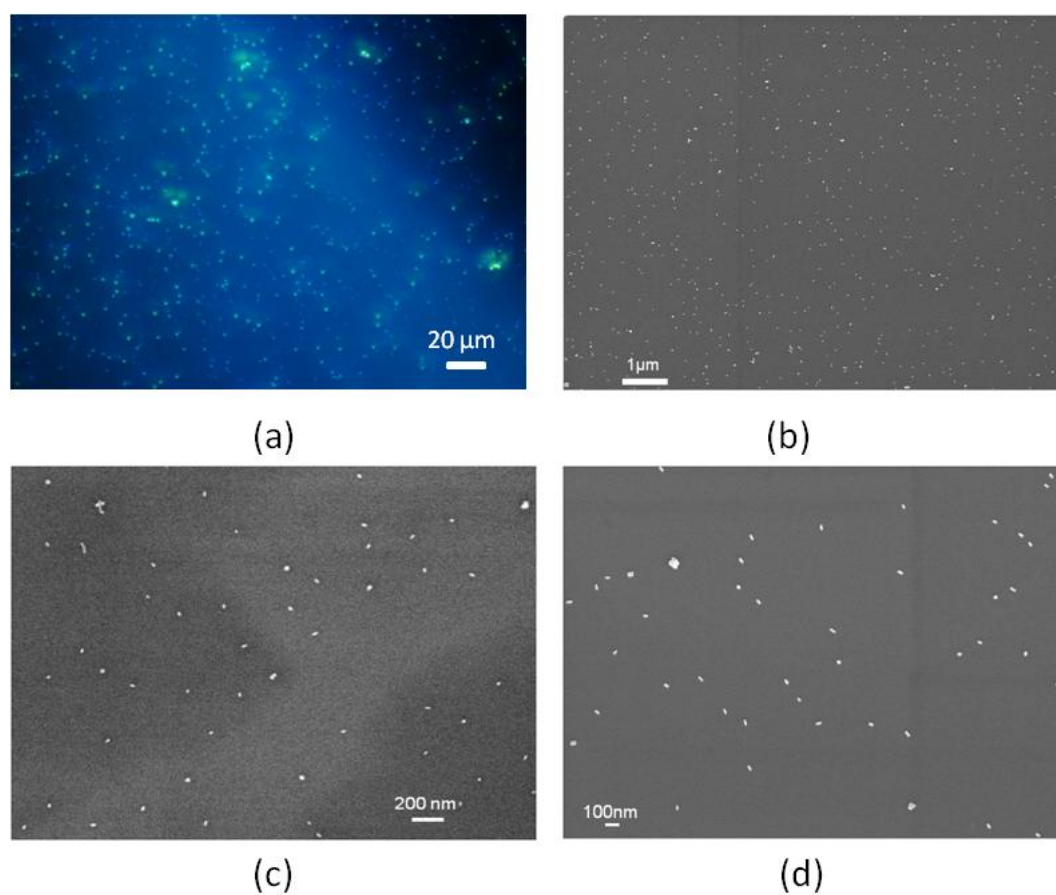2.2 Linear chains of twisted Au NRs. with interparticle distance ~ 250 nm

Fig. S5. Morphology and structure of the lipid-based linear chains of Au NRs (aspect ratio ~ 2.7). (a) Optical microscope (dark-field) images obtained during the drying process of the solution sample; (b-d) SEM images obtained from the dried samples without gold sputter-coating treatment.

2.3 Twisted chains of Au NRs (aspect ratio ~ 2.7) with the interparticle distance of ~ 320 nm or ~ 480 nm
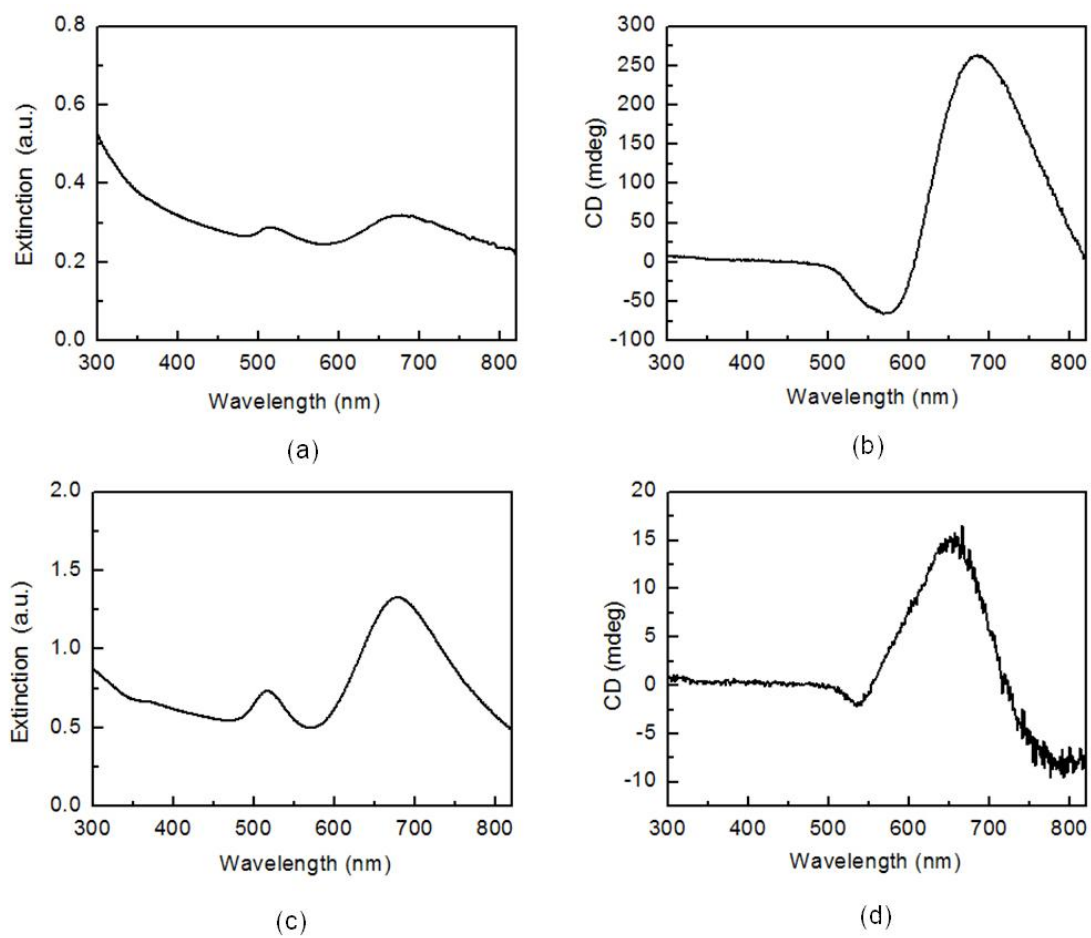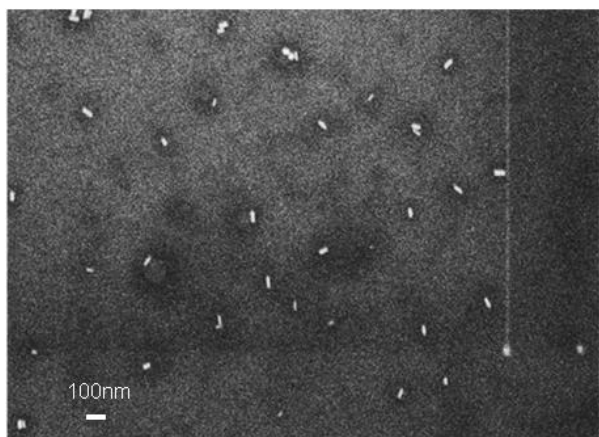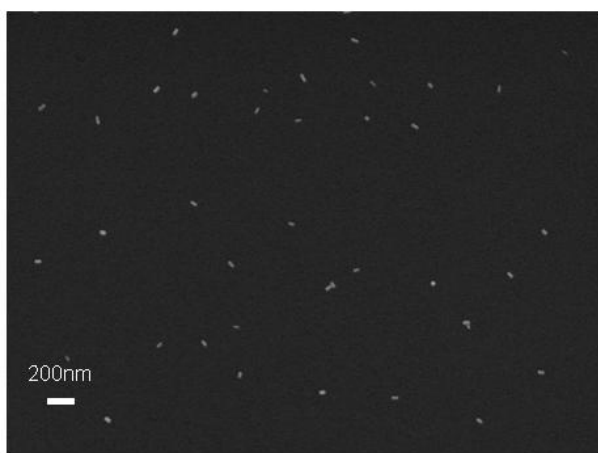
Fig. S6. Extinction and CD spectra acquired from twisted chains of Au NRs (aspect ratio 2.7) solution with interparticle distance $D \sim 320$ nm (a, b), and $D \sim 480$ nm (c, d). The corresponding concentration of Au NRs in the two samples was ~ 0.4 nM and ~ 0.8 nM, respectively.

(a)

(b)

Fig. S7. SEM images acquired from dried samples (without gold sputter-coating) of the twisted chains of Au NRs (aspect ratio ~ 2.7) with interparticle distance 320 ± 46 nm (a) and 480 ± 52 nm (b).

2.4 Twisted chains of Au NRs with different aspect ratios.
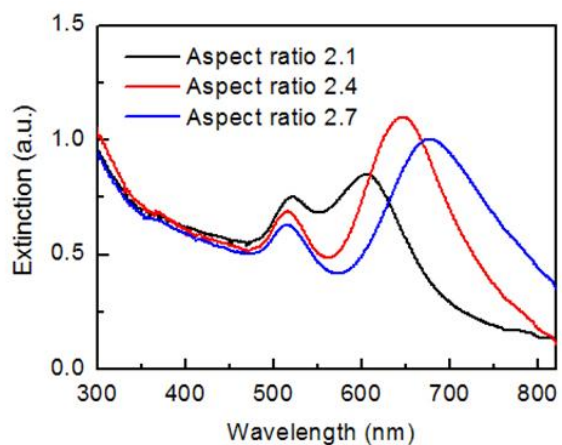
(a)
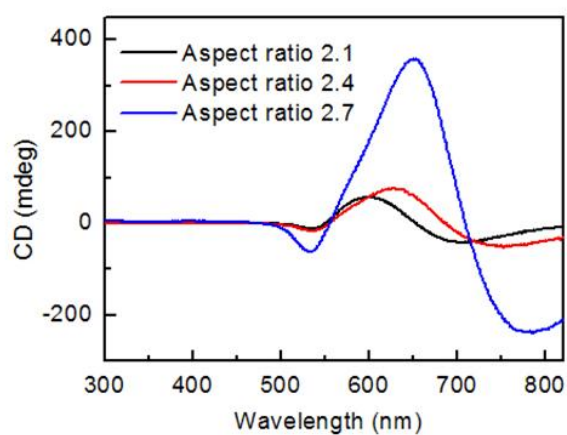
(b)

Fig. S8. Extinction (a) and CD (b) spectra of the twisted chains of Au NRs with different aspect ratios (before the centrifugation treatments). The concentration of Au NRs in the three samples with aspect ratios ~ 2.1, ~ 2.4 and ~ 2.7 were ~ 0.9 nm, ~ 0.8 nM, and ~ 0.8 nM, respectively.

Fig. S9. Curves of the anisotropy factors acquired for the twisted chains of Au NRs with an aspect ratio of ~ 2.1 (black solid line), ~ 2.4 (red solid line), and ~ 2.7 (blue solid line), respectively.
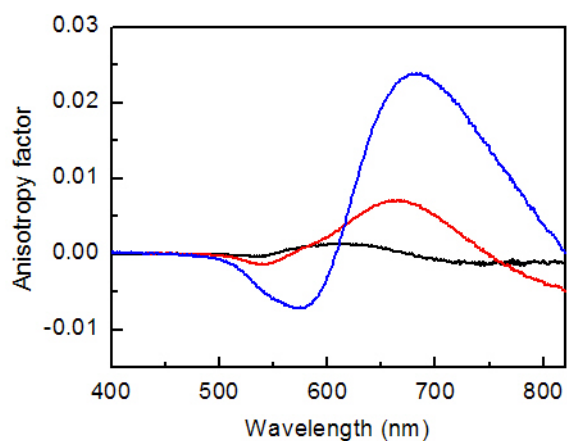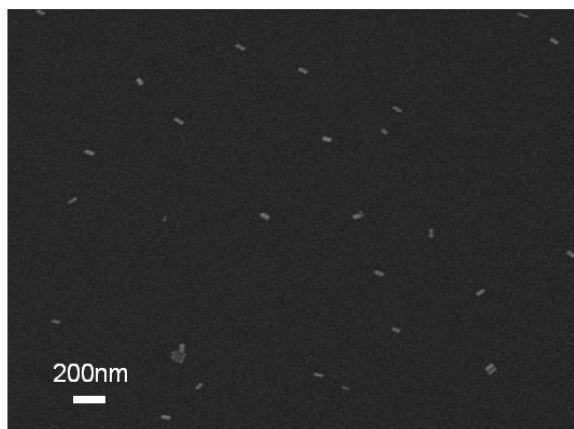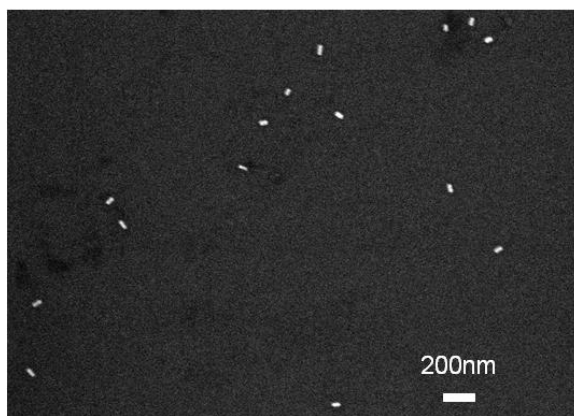

(a)

(b)

Fig. S10. Representative SEM images of the dried samples (without gold sputter-coating) of the twisted chains of Au NRs after centrifugation treatment. The aspect ratios of Au NRs in the two chains were ~ 2.1 (a) and ~ 2.4 (b), respectively.

Simulation Section::

Theoretical modeling of chiral dimer of gold nanorods.

1. The coupled-dipole approximation method.

The coupled-dipole approximation[2-6] is widely used to calculate circular dichroism (CD), and in particular the interaction between isolated elements of a system.[2, 3, 7-11] This method was first introduced by DeVoe et al to study the optical properties of molecular aggregates in a solution.[2, 3] And then the coupled-dipole approximation has found application to describe the scattering properties of plasmonic nanoparticles.[12, 13] In this model, each NP is described as an electric dipole, which is validated in the far-field coupling scenario, where the particle size is much small than the wavelength, and the interparticle distance is large compare to the particle size. By using this model, Govorov[14] and Liz-Marzán[15] has predicted successfully the induced plasmonic CD in a helical geometry of gold NPs/NRs complex.

Herein we followed a simple chiral model of two prolate ellipsoids of gold nanoparticles proposed by Auguié and co-workers,[16] by which our chiral plasmonic system was idealized to be a dimer of two dipoles that oriented along the long axis of each ellipsoid. The electric dipole moment $\vec{p}_i$ of individual nanorods is given by:

$$\vec{p}_i = \vec{\alpha}_i \cdot \left(\vec{E}_{inc,i} + \sum_j \vec{E}_{dip,j} \right) \tag{1}$$

where $\vec{\alpha}_i$ is the polarisability tensor that describes the individual nanorods,[17] $\vec{E}_{inc,i}$ is the incident field from left-handed or right-handed circularly polarized light acting on the

nanorods, and $\vec{E}_{dip,j}$ is the scattered field from other nanorods. For the scattered field of

particle j acting on particle i, we can write it as dipole field in Green function:[18]

$$\vec{E}_{dip,j} = \omega^2 \mu \mu_0 \vec{\vec{G}}(\vec{r}_i, \vec{r}_j) \cdot \vec{p}_j$$

$$\vec{\vec{G}}(\vec{r}_i, \vec{r}_j) = \frac{\exp(ikR)}{4\pi R}\left[\left(1 + \frac{ikR-1}{k^2 R^2}\right)\vec{\vec{I}} + \frac{3 - 3ikR - k^2 R^2}{k^2 R^2}\frac{\vec{R}_{ij}\vec{R}_{ij}}{R^2}\right] \tag{2}$$

where R is the absolute value of the vector $\vec{R}_{ij} = \vec{r}_i - \vec{r}_j$ and $\vec{R}_{ij}\vec{R}_{ij}$ denotes the outer

product of $\vec{R}_{ij}$ with itself. $\vec{r}_i$ and $\vec{r}_j$ are the position of particle i and particle j. Combing

the Equation (1) and (2) with considering all the possibility of i and j, the scattering problem

can be solved self-consistently for the electric dipole moment $\vec{p}_i$, from which we can

calculate the extinction cross-section

$$\sigma_{ext} = \frac{4\pi k}{|\vec{E}_{inc}|^2}\sum_i \left(\vec{E}_{inc,i}^{\ *} \cdot \vec{p}_i\right) \tag{3}$$

The circular dichroism (CD) cross sections are given by the difference in extinction for

left-handed (LH) and right-handed (RH) circularly polarized light,

$$\sigma_{CD} = \left\langle \sigma_{ext,LH} - \sigma_{ext,RH}\right\rangle_\Omega \tag{4}$$

where the averaging over the solid angle Ω, is needed since complexes are in a solution and

have random orientations.

As shown in Equation (2), the Green's function $\vec{\vec{G}}_{i,j}$ has terms in $(kR)^{-1}$, $(kR)^{-2}$ and

$(kR)^{-3}$, which corresponding to the far field ($R \gg \lambda$), intermediate-field ($R \approx \lambda$) and near

field ($R \ll \lambda$), $\vec{G} = \vec{G}_{NF} + \vec{G}_{IF} + \vec{G}_{FF}$. The properties of the circular dichroism (CD) will be

dominated by different part with the different interparticle distance. The polarisability tensor

strongly dependents on aspect ratio, which induces shaped CD spectra with varied aspect ratio

of Nanorods (See Fig. S11).

During the numerical simulation, we set here the twist angle $\theta = 135^{\circ}$ and the angle between the long axis of nanorod and the helical axis $\Phi_{NR1} = \Phi_{NR2} = 90^{\circ}$. Corresponding to the plasmon-plasmon interaction of Au NRs mediated by intermediate- and far-field couplings, the values of D in the range of $90 - 1500$ nm were chosen in our simulations. In addition, for the aqueous environment of the twisted chains of gold nanorods, a typical value of refractive index of water at room temperature ($n = 1.333$) was used in the simulations.
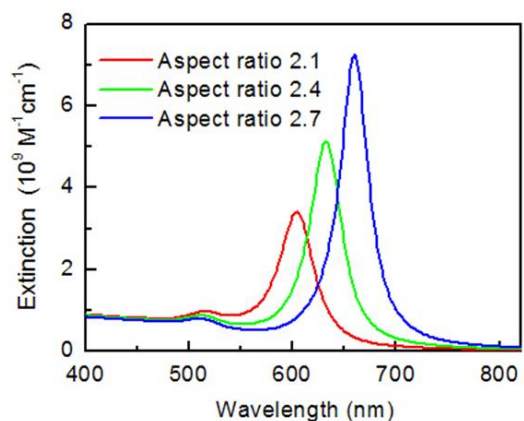
(a)
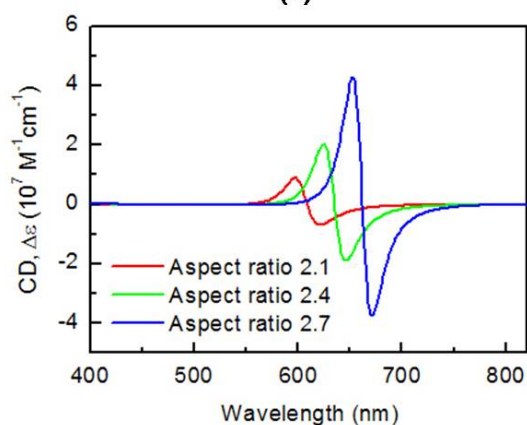
(b)
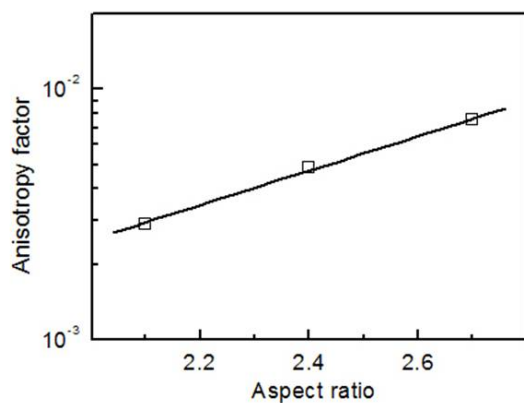
(c)

Fig. S11. Extinction (a) and CD (b) spectra of twisted chains of Au NRs with different aspect ratios at 2.1 (red solid line), 2.4 (green solid line), and 2.7 (blue solid line); (c) Anisotropy factor of twisted chains of Au NRs with different aspect ratios.

2. Simple theoretical analysis for dimer-dipole system.

To make a simple theory analysis, our system can be idealized to a dimer of two dipoles. For a two dipole model, the CD couplet can be expressed as[19]

$$\Delta\varepsilon(\lambda) \propto \pm\Gamma(\lambda)V_{12}R_{\pm} \propto \pm\Gamma(\lambda)\frac{\mu_1^2\mu_2^2}{r_{12}^2}\Omega(\alpha,\beta,\gamma) \tag{5}$$

where Γ, V_{12} and $R_{\pm}$ are corresponding to three factors related to the dispersive couplet shape, the interaction potential and the rotational strength respectively. μ_1, μ_2 and r_{12} are the intensities and mutual distance of the two transition dipoles, while $\vec{e}_1$, $\vec{e}_2$ and $\vec{e}_{12}$ are the corresponding unit vectors which will be used in the following. Ω is the geometric term as a function of three angle α, β and γ which are corresponding to the angle between $\vec{e}_1$ and $\vec{e}_{12}$, $\vec{e}_2$ and $\vec{e}_{12}$, $\vec{e}_2$ and $\vec{e}_2$. In general, the interaction potential only considered the case of near-field coupling with no-retarded interaction, as $V_{12} = \mu_1\mu_2/r_{12}^3[\vec{e}_1\cdot\vec{e}_2 - 3(\vec{e}_1\cdot\vec{e}_{12})(\vec{e}_2\cdot\vec{e}_{12})]$, which is obviously unsuitable for large distance here. In this system, the intermediate field, the far field and the retarded effect should be considered. With this consideration, we can get the interaction potential through Coulomb interaction. We have interaction Hamiltonian as: [18]

$$H_{int} = q\phi(0,t) - \vec{\mu}\cdot\vec{E}(0,t) - \vec{m}\cdot\vec{B}(0,t) - [\vec{\vec{Q}}\nabla]\cdot\vec{E}(0,t) - ...$$

Only the second term works here, thus

$$H_{int} = -\vec{\mu}_1\cdot\vec{E}_2 - \vec{\mu}_2\cdot\vec{E}_1 = -\vec{\mu}_1\cdot\omega^2\mu\mu_0\vec{\vec{G}}_2\cdot\vec{\mu}_2 - \vec{\mu}_2\cdot\omega^2\mu\mu_0\vec{\vec{G}}_1\cdot\vec{\mu}_1$$

Finally, the interaction potential will be

$$V_{12} = H_{int} \propto -\frac{\omega^2\mu\mu_0\exp(ikR)}{4\pi R}\left[\left(1+\frac{ikR-1}{k^2R^2}\right)(\vec{\mu}_1\cdot\vec{\mu}_2) + \frac{3-3ikR-k^2R^2}{k^2R^2}\frac{(\vec{\mu}_1\cdot\vec{R}_{12})(\vec{\mu}_2\cdot\vec{R}_{12})}{R^2}\right]$$

which can be rewritten as

$$V_{12} = V_{12-NF} + V_{12-IF} + V_{12-FF} \tag{6}$$

Here,

$$V_{12-NF} \propto \frac{\mu_1 \mu_2 \exp(ikr_{12})}{4\pi\varepsilon_0 r_{12}^3}\left[\vec{e}_1 \cdot \vec{e}_2 - 3(\vec{e}_1 \cdot \vec{e}_{12})(\vec{e}_2 \cdot \vec{e}_{12})\right]$$

$$V_{12-IF} \propto -\frac{ik\mu_1 \mu_2 \exp(ikr_{12})}{4\pi\varepsilon_0 r_{12}^2}\left[\vec{e}_1 \cdot \vec{e}_2 - 3(\vec{e}_1 \cdot \vec{e}_{12})(\vec{e}_2 \cdot \vec{e}_{12})\right]$$

$$V_{12-FF} \propto -\frac{\mu_1 \mu_2 k^2 \exp(ikr_{12})}{4\pi\varepsilon_0 r_{12}}\left[\vec{e}_1 \cdot \vec{e}_2 - (\vec{e}_1 \cdot \vec{e}_{12})(\vec{e}_2 \cdot \vec{e}_{12})\right]$$

V_{12-NF}, V_{12-IF} and V_{12-FF} corresponding to the interaction potential of near-field, intermediate-field and far-field. k is the wave vector and ε_0 is the vacuum permittivity. With the rotational strength $R_{\pm} = \mathrm{Im}(\vec{p} \cdot \vec{m}) \propto \mp \vec{r}_{12} \cdot \vec{\mu}_1 \times \vec{\mu}_2$, where $\vec{p}$ and $\vec{m}$ stand for the electric and magnetic dipole moments, finally the CD couplet can be expressed as

$$\Delta\varepsilon(\lambda) \propto \pm\Gamma(\lambda)\exp(ikr_{12})\mu_1^2\mu_2^2\left(\frac{1}{r_{12}^2}\Omega_{NF} - \frac{ik}{r_{12}}\Omega_{IF} - k^2\Omega_{FF}\right) \tag{7}$$

where Ω_{NF}, Ω_{IF} and Ω_{FF} are the geometry factor of near-field, intermediate-field and far-field respectively. It should be noted that $\Omega_{NF} = \Omega_{IF}$. The term $\mu_1^2\mu_2^2$ reveals that the CD couplet intensity is directly proportional to the fourth power of the dipole strength. The term $\exp(ikr_{12})$ shows that the intensity of CD will oscillate with the interparticle distance r_{12}, and since $\Omega_{NF} = \Omega_{IF}$ in $1/r_{12}^2 \cdot \Omega_{NF} - ik/r_{12} \cdot \Omega_{IF}$, the contribution of intermediate field will be stronger than near-field when $r_{12} > 1/k$. That's why the CD strength displays a damped oscillation in Fig. S12. For the contribution of far field part, long enough of distance and suitable configuration are needed. In fact, suitable configurations of these particles are always needed to generate the nonzero geometry factor Ω in chiral structure.
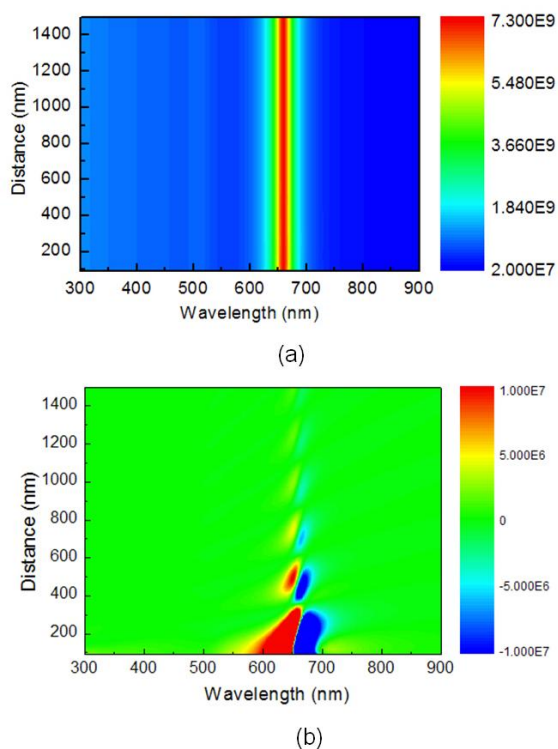
(a)

(b)

Fig. S12. Color plot of simulated extinction (a) and CD (b) spectra of twisted chains of Au NRs (aspect ratio 2.7) as a function of the interparticle distance.
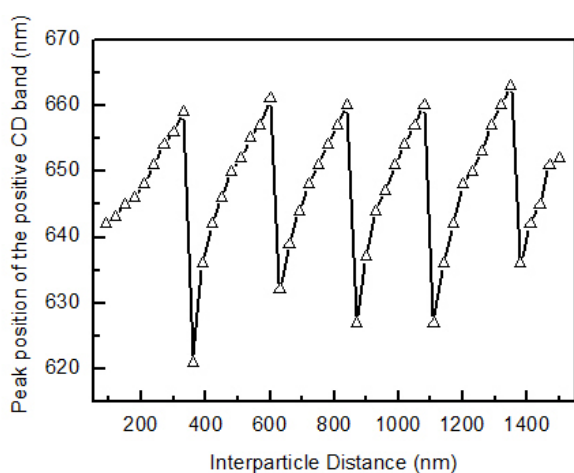

Fig. S13. A sawtooth wave like behavior in the peroidically red-shift of the spectral position (peak position of the positive CD band) as the interpartciel distance increases.

REFERENCES

1. S. Link and M. A. El-Sayed, *J. Phys. Chem. B,* 2005, **109**, 10531.

2. H. DeVoe, *J. Chem. Phys*., 1965, **43**, 3199.

3. H. DeVoe*, J. Chem. Phys., 1964,* **41***, 393.*

4. B. Draine and P. Flatau, *J. Opt. Soc. Am. A,* 1994, **11**, 1491.

5. B. Draine, *Astrophys. J.,* 1988, **333**, 848.

6. M. A. Yurkin, A. G. Hoekstra and J. Quant. *Spectrosc. Ra.,* 2007, **106**, 558. IX Conference on Electromagnetic and Light Scattering by Non-Spherical Particles.

7. M. Kim, L. Ulibarri, D. Kelle and M. F. Maestre, *J. Chem. Phys.,* 1986, **84**, 2981.

8. C. Noguez, *Phys. Rev. 200*6, **73**, 1.

9. C. E. Roman-Velazquez, C. Noguez and I. L. Garzon, *J. Phys. Chem. B,* 2003**, 107**, 12035.

10. C. Noguez and I. L. Garzon, *Chem. Soc. Rev.,* 2009, **38**, 757.

11. Z. Fan and A. O. Govorov, *Nano Lett.,* 2010, **10**, 2580.

12. G. C. Schatz and R. P. V. Duyne, *J. Chem. Phys.,* 1995, **103**, 869.

13. G. C. Schatz, L. Jensen, K. L. Kelly and, A. A. Lazarides, *J. Clust. Sci.*, 1999, **10**, 295.

14. Z. Fan and A. O. Govorov, *Nano Lett.,* 2010, **10**, 2580.

15. A. Guerrero-Martínez, B. Auguié, J. L. Alonso-Gómez, Z. Dzolic, S. Góbmez-Grana, M. Zinic, M. M. Cid and L. M. Liz-Marzán, *Angew. Chem. Int. Ed*., 2011, **50**, 5499.

16. B. Auguié, J. L. Alonso-Gomez, A. Guerrero-Martínez and L. M. Liz-Marzan, *J. Phys. Chem. Lett.,* 2011, **2**, 846.

17. H. Kuwata, H. Tamaru, K. Esumi and K. Miyano, *Appl. Phys. Lett.* 2003, **83**, 4625.

18. L. Novotny and B. Hecht, Principles of Nano-Optics, Cambridge University Press, Cambridge: England, 2006.

19. N. Berova, L. D. Bari and G. Pescitelli, *Chem. Soc. Rev.,* 2007, **36**, 914.